

Multi-Fin Bulk FinFET Characteristic Fluctuation Induced by Process Variation and Random Dopant

Chieh-Yang Chen, Yu-Yu Chen, and Yiming Li*

Parallel and Scientific Computing Laboratory, Department of Electrical and Computer Engineering,
National Chiao Tung University, 1001 Ta-Hsueh Road, Hsinchu 300, Taiwan
e-mail: ymli@faculty.nctu.edu.tw

I. INTRODUCTION

Device scaling has suffered sizeable statistical variation in device parameter and has increased the short-channel effect (SCE) [1-2]. To overcome the variation and SCE, 3D transistor, such as bulk FinFET in sub-22-nm has been one of competitive solutions [3-4]. Impurity dopants are continuously adopted for tuning device characteristics. Recent simulations have been reported for single SOI and bulk FinFET device's characteristic fluctuation [5-7]. However, the multi-fin bulk FinFET's random dopants fluctuation (RDF) and the process variation effect (PVE) including the variations of silicon fin's fin height (Hf), fin width (Wf), and gate length (Lg) have not been clearly explored yet.

In this work, 16-nm-gate HKMG multi-fin bulk FinFET devices are simulated for both the RDF and PVE. Experimentally validated 3D quantum-mechanically corrected device simulation is intensively performed to statistically analyze the impact of RDF and PVE on the device characteristic fluctuation.

II. SIMULATION AND RESULTS DISCUSSION

As shown in Fig. 1(a), we study the single-fin and multi-fin (four fins) bulk FinFET in which both the channel length and device width are 16 nm and silicon fin height is 32 nm. We randomly generate 1,327 dopants in a large cube of $(96 \text{ nm})^3$, in which the equivalent doping concentration is $1.5 \times 10^{18} \text{ cm}^{-3}$. The large cube is partitioned into sub-cubes. The number of dopants in the sub-cubes may vary from 0 to 14, and the average dopant number is 6. (Similarly, for the FinFET's Hf of 32 nm; devices are with 2,654 dopants in $96 \times 192 \times 96 \text{ nm}^3$ cube and average dopant number is 12) These sub-cubes are then mapped into the device channel region for 3D device simulation, as shown in plot Fig. 1(a). Fig. 1(c) shows the diagram of the fin's process variation. And, the fin's variation includes the Hf, Wf, and Lg which varies follow the table in Fig. 1(c).

As shown in Figs. 2(a) and 2(b), the single-fin's I_D - V_G characteristics are fluctuated by the RDF and PVE, respectively. The PVE varying

with respect to each factor the Hf, the Lg, and the Wf, is further shown in Figs. 2(c)-(e). The solid line shows the nominal case with a channel doing of $1.5 \times 10^{18} \text{ cm}^{-3}$ and V_{th} is experimentally calibrated to 140 mV. Similarly, as shown in Fig. 3, we simulate the four-fin's I_D - V_G characteristic for the devices suffering the RDF and PVE. We stimulate the σV_{th} resulting from the RDF and PVE, as shown in Fig. 4. Compared with the single fin device, the multi-fin device can suppress the V_{th} fluctuation of RDF about 48% owing to the increase of fin numbers and the enhanced screening effect. The more we increase the fin number, the more we suppress the fluctuation; nevertheless, the improvement will be limited by the geometry aspect of fin which should be subject to further investigation. For the suppression of PVE, it is merely 10% due to different fin shape. As shown in Fig. 5, we list the normalized σV_{th} , σI_{on} , and σI_{off} for both the cases of single- and multi-fin resulting from the PVE and RDF. The multi-fin structure can effectively suppress the fluctuation from RDF and PVE on V_{th} and I_{on} , but the variation of I_{off} is increased for the case of multi-fin devices.

III. CONCLUSIONS

In this work, we have statistically performed the 3D device stimulation to estimate the multi-fin device's fluctuation. The results indicate that the multi-fin device can successfully suppress RDF by 48% and PVE by 10% on σV_{th} , compared with the single-fin device.

ACKNOWLEDGEMENT

This work was supported in part by the Taiwan National Science Council (NSC) under Contract No. NSC-101-2221-E-009-092 and a 2012-2013 tsmc grant.

REFERENCES

- [1] Y. Li et al., in: *IEDM Tech. Digest* 171(2012).
- [2] Y. Li et al., *IEEE TED* 57 (2010) 437.
- [3] K. J. Kuhn et al. in: *IEDM Tech. Digest* 171(2012).
- [4] C.-H. Lin et al., in: *Proc. Symp. VLSI Tech.*, 2.3 (2012).
- [5] H.-W. Su et al., in: *Proc. IEEE DRC* 109 (2012).
- [6] X. Wang et al., in: *IEDM Tech. Digest* 103 (2011).
- [7] H.-W. Cheng et al., in: *Proc. IEEE SISPAD* 287 (2011).

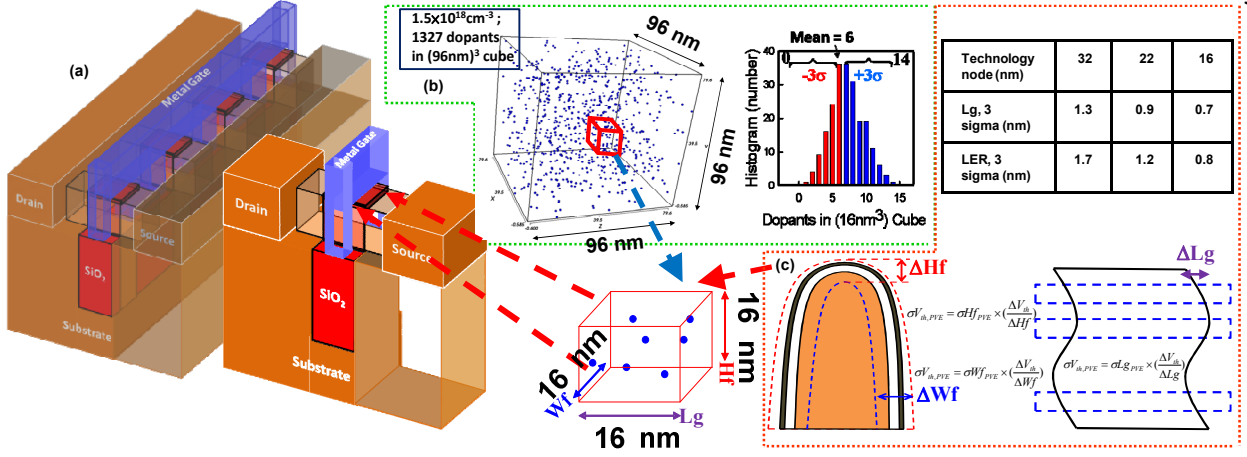


Fig. 1. (a) An illustrate of the device structure for both the single- and Multi-fin. (b) We randomly generate 1,327 dopants in a large cube of $(96 \text{ nm})^3$, in which the equivalent doping concentration is $1.5 \times 10^{18} \text{ cm}^{-3}$. The large cube is partitioned into sub-cubes. The number of dopants in the sub-cubes may vary from 0 to 14, and the average dopant number is 6. (Similarly, for FinFET AR2 devices: 2,654 dopants in $96 \times 192 \times 96 \text{ nm}^3$ cube and average dopant number is 12). The AR2 is defined as Fin height / Fin width = 2. These sub-cubes are then mapped into the device channel region for 3D device simulation, as shown in plot (a). (b) The diagram of fin's process variation. Fin's variation includes the Hf, Wf, and Lg which varies follow the inset table.

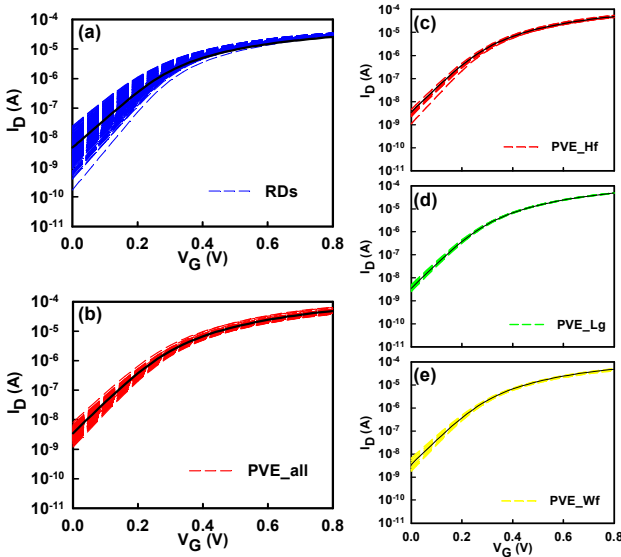


Fig. 2. The single-fin's I_D - V_G characteristics for (a) RDF, (b) PVE. (c) Hf, (d) Lg, and (e) Wf are each factor's impact. The solid line in each plot shows the nominal case with a channel doing $1.5 \times 10^{18} \text{ cm}^{-3}$ and the V_{th} is equal to 140 mV.

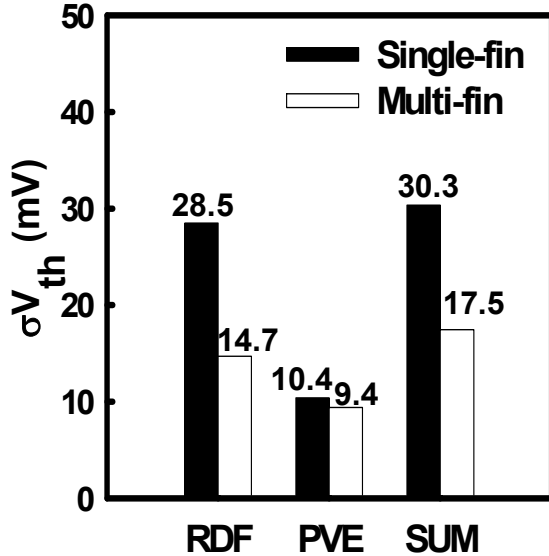


Fig. 4. Plot of the σV_{th} calculated from the devices with the RDF, PVE, and their statistical sum: $(\sigma^2 V_{th,RDF} + \sigma^2 V_{th,PVE})^{0.5}$.

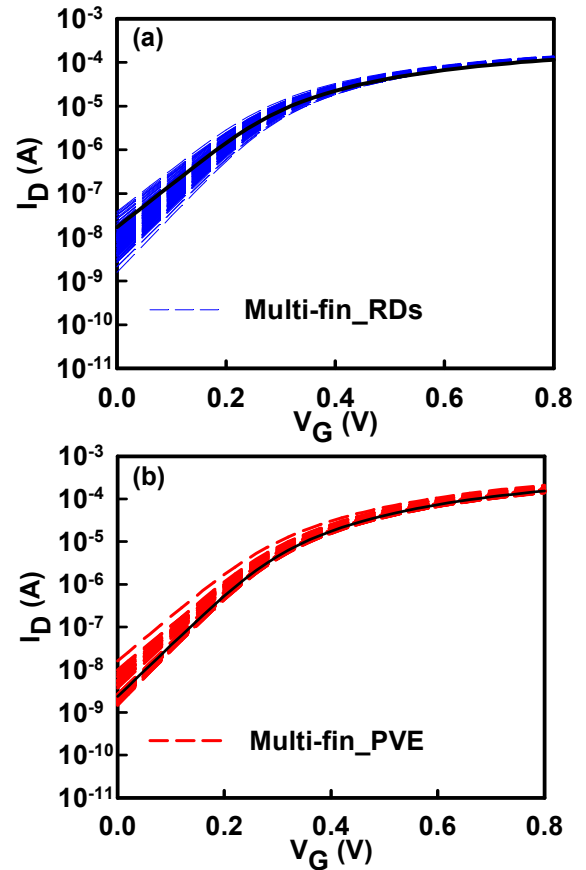


Fig. 3. The multi-fin's I_D - V_G characteristics for both the (a) RDF and (b) PVE, where the fin number is 4.

	Normalized $\sigma_{V_{th}}$ (%)	Normalized $\sigma_{I_{on}}$ (%)	Normalized $\sigma_{I_{off}}$ (%)
PVE Hf	5.3	5.5	20.7
PVE Lg	2.5	0.5	12.0
PVE Wf	4.3	4.3	23.1
PVE all	7.4	12.0	37.7
RDF	20.4	4.2	99.3
Multi-fin RDF	9.7	3.2	64.8
Multi-fin PVE	6.8	6.2	65.3

Fig. 5. The first 4 rows are the normalized σV_{th} , σI_{on} , and σI_{off} of the single-fin and the last two rows are the multi-fin's PVE and RDF. The multi-fin structure effectively suppresses the fluctuation from both the RDF and PVE on V_{th} and I_{on} .